

Process Modeling Based on Atomistic Understanding for State of the Art CMOS Device Design

S. Chakravarthi*, M. Diebel*, P.R. Chidambaram*, S. Ekbote*,
S.T. Dunham**, C.F. Machala*, S. Johnson*

* Silicon Technology Development, Texas Instruments Inc.
Dallas, TX 75243. s-chakravarthi@ti.com

** Department of Electrical Engineering, University of Washington, Seattle, WA 98105.

ABSTRACT

Atomistic modeling methods are emerging as a powerful tool to understand the physical behavior of complex systems. However, continuum process simulators are the core of state of the art TCAD simulators and substantial challenges must be overcome to make effective use of atomistic techniques. As device dimensions shrink into the sub 100 nm regime, one of the problems faced by device designers is the diffusion of phosphorus (P) from the source/drain region into extensions due to reduction of the source/drain sidewall distance. We use this problem to illustrate how accurate and physical process models can help understand these issues. In particular, we develop a continuum model for phosphorus (P) and fluorine (F) diffusion from our understanding at an atomic level. These models are then calibrated to predict more complex interactions between phosphorus and fluorine.

Keywords: Phosphorus diffusion, Fluorine diffusion, modeling, CMOS

1 Diffusion of Phosphorus In Silicon

Phosphorus is one of the key elements used in front end processing of modern CMOS devices. It is also one of the most challenging dopants to model due to the anomalous kink and tail profile [1]. Early experimental results on phosphorus diffusion suggested a vacancy dominated mechanism [2]. Further experiments on phosphorus diffusion under intrinsic conditions indicate the importance of interstitial assisted mechanism [3]. Recent *ab-initio* calculations found intrinsic phosphorus diffusion is dominated by an interstitial (I) mechanism [4]. Pair diffusion models considering an attractive potential between the dopant and point defects are well accepted for modeling diffusion in silicon [3]. For an interstitial mechanism this implies diffusion of a phosphorus interstitial (PI) pair. However, for a vacancy mediated diffusion step, there is a fundamental requirement that the vacancy must move away to at least a third nearest neighbor site and return to the dopant from a different direction. This arises due to the basic complication that a dopant moving into a vacant site leads to a vacancy moving in the opposite direction and

subsequently exchanging places with a vacancy does not lead to a net displacement. The dopant vacancy pair thus partially dissociates and reforms many times before fully dissociating. The exact form of the dopant vacancy interaction potential will hence have a significant impact on the dopant diffusivity by this mechanism. Infact, *ab-initio* calculations show relatively long-range interactions between dopants and vacancies (out to at least tenth nearest neighbor distances) [5]. The presence of such long-range interactions opens the door for relatively complex interactions among multiple dopants with multiple vacancies, particularly at high doping levels. Lattice Monte Carlo simulations using such *ab-initio* results have predicted a large increase in dopant diffusivities at high dopant concentrations [6] and agree with experimental results [7]. This arises due to interactions of a vacancy with multiple dopants leading to a net decrease in migration barrier for the PV pair. An example of this phenomenon is illustrated in Fig. 1. Interaction with a second dopant atom reduces the net activation energy for pair diffusion associated with third to second nearest neighbor transitions, resulting in a net increase in dopant diffusivity. In contrast, simple pair diffusion models do not consider long range interaction between dopants and point defects and correction terms are added.

Thus, in our continuum simulations [8] we use a model where intrinsic diffusion is mediated almost exclusively by interstitials whereas higher concentration diffusion is mediated via vacancies. Fig. 2 compares our model calibrated to high dose phosphorus diffusion data. We plot the diffusivities used in our simulations in Fig. 3 and find a similar enhanced high concentration diffusion. This agrees well with our understanding from Lattice Monte Carlo simulations and previous experimental results [6], [7] that show a polynomial increase in diffusivity (D_P) with concentration (C_P) ($D_P \propto C_P^n$; $n = 3 - 4$).

2 Diffusion of Fluorine In Silicon

Fluorine diffuses anomalously in silicon [9]. A characteristic of fluorine diffusion is the unusual shape of the diffused fluorine profiles. Instead of the normal gaussian diffusion, fluorine exhibits an immobile profile that shifts towards the surface (see Fig. 4). Such a behav-

ior indicates the formation of strongly bound fluorine complexes, since ab-initio calculations give a migration barrier of only 0.7-1.3 eV for an interstitial fluorine (F_i) indicating it to be a highly mobile [10],[11]. Further, the addition of fluorine to boron implants typically retards boron diffusion [12]. The mechanism for this retardation is however not clear.

Recently *ab-initio* calculations have been used to explore and understand fluorine diffusion [13]. These density functional theory based calculations find stable fluorine vacancy complexes (F_nV_m) with high binding energies. Fig. 5 shows the binding energies associated with these F_nV_m complexes as calculated by this technique. In particular, they find a very strong binding for F_3V and F_6V_2 clusters. This is because fluorine saturates the dangling bonds associated with small vacancy clusters. The addition of fluorine atoms into clusters also leads to lattice distortion due to repulsion between the fluorine atoms. Consequently, this makes the $F_{3n}V$ clusters more stable relative to $F_{3n+1}V$ clusters. The larger F_6V_2 cluster is stable even in the presence of an interstitial super-saturation. A multi-cluster continuum model incorporating these calculations was developed incorporating all the reaction pathways. This model exhibits anomalous diffusion similar to experimental data [13]. This arises due to fluorine vacancy complexes dissolving in the deeper interstitial rich region, but stabilized in the vacancy rich near surface region. This multi-cluster model is however too complex for use in an industrial process simulator. We analyze this model to develop a simpler form of this fluorine model. Fig. 6 illustrates the time evolution of different F_nV_m clusters using this model. From Fig. 6 it is clear, the F_3V cluster forms rapidly during the initial stage of implant annealing. Further, evolution of fluorine profile occurs by the dissolution of F_3V cluster into the rapidly migrating fluorine interstitial (F_i). Some of these F_3V clusters also ripen into more stable F_6V_2 clusters. Hence, we implemented a simple reaction ($F_3V + I \rightleftharpoons 3F_i$) in our process simulator and calibrated it to data. Fig. 7 shows a similar anomalous diffusion of the fluorine profile matched well by the model. During the anneal, the F_3V dissolution is driven by the interstitials deeper in the bulk leading to an apparent anomalous diffusion of the fluorine. The consumption of interstitials by the dissolution of F_3V and F_6V_2 clusters reduces the net interstitial super-saturation. Hence the presence of fluorine is expected to retard the diffusion of interstitial diffusing elements like boron and phosphorus in the absence of B-F or P-F interactions.

3 Phosphorus/Fluorine Interactions

Preliminary *ab-initio* calculations find very weak binding between phosphorus and fluorine. We thus expect the primary interaction to be due to changes in point

defect concentrations. To study phosphorus-fluorine interactions, we co-implanted phosphorus and fluorine at varying doses and energies. We find a strong retardation of the phosphorus tail diffusion with almost no change in the shoulder diffusion behavior. Simulations match this trend very well (Fig. 8). The fluorine atoms form fluorine vacancy complexes leading to a net decrease in interstitial super-saturation. The phosphorus shoulder is unaffected, since phosphorus diffusion is mediated primarily via vacancies at these high concentrations. This also confirms our understanding of both phosphorus and fluorine diffusion.

4 Applications of Process Models

We now apply our model to look at NMOS transistors with gate lengths of 50nm. The problem of excessive diffusion of the source/drain phosphorus is represented in Fig. 9. Fig. 10 shows addition of fluorine can decrease phosphorus diffusion into the channel. Electrical parameter results show a similar trend supporting our model results.

5 Conclusions

Designing transistors at the nanometer regime is a challenging task and requires significant front end optimization. Development of continuum process models based on atomistic level understanding help to successfully predict dopant redistribution during silicon thermal processing. These models are then successfully used to optimize performance of state of the art transistors.

REFERENCES

- [1] M. Yoshida *Jap. J. Appl. Phys.* **18**, 479 (1979).
- [2] R.B. Fair and J.C.C. Tsai in *J. Electrochem. Soc.* **124**, 1107 (1977).
- [3] P. Fahey, P.B. Griffin, and J.D. Plummer, *Rev. Mod. Phys.* **61**, 289 (1989).
- [4] X.Y. Liu, W. Windl and M.P. Masquelier, *Mat. Res. Soc. Symp. Proc.* **717**, C4.7.1 (2002).
- [5] O. Pankratov, H. Huang, T.D. de la Rubia and C. Mailhot *Phys. Rev. B* **76**, 4753 (1996).
- [6] M. Bunea and S.T. Dunham *J. Comp. Aid. Des.* **5** 81 (1998).
- [7] A.N. Larsen, K.K. Larsen, P.E. Andersen, and B.G. Svensson, *J. Appl. Phys.* **73** (2), 691 (1993).
- [8] T-SUPREM4 2001.4 *Avant! Corp.*
- [9] S.P. Jeng, T.P. Ma, R. Canteri, M. Anderle and G.W. Rubloff *Appl. Phys. Lett.* **61** 1310 (1992).
- [10] C.G. Van de Walle, F.R. McFeely, and S.T. Pantelides, *Phys. Rev. Lett.* **61**, 1867 (1988)
- [11] A. Taguchi and Y. Hirayama, *Solid State Commun.* **116**, 595 (2000).
- [12] D.F. Downey, J.W. Chow, E. Ishida, and K.S. Jones *Appl. Phys. Lett.* **73** (9), 1263 (1998).

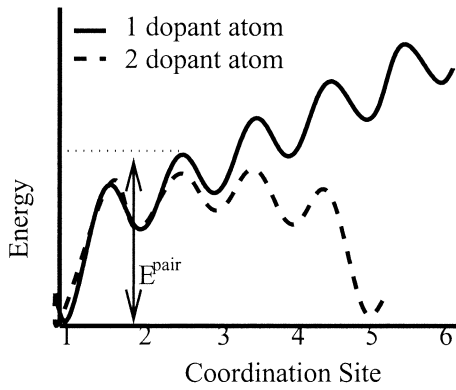


Figure 1: Schematic illustration of vacancy energy as a function of position away from a dopant atom. The presence of a second dopant atom can lower the vacancy energy as a function of position due to overlapping potentials. This decreases the pair migration energy in the presence of the second dopant atom.

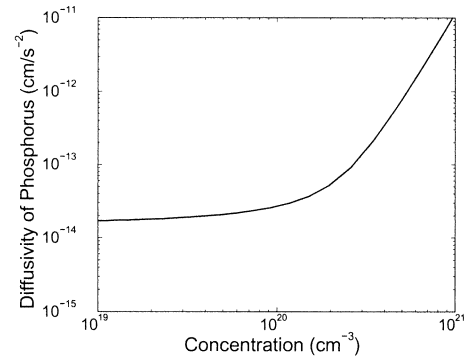


Figure 3: Phosphorus diffusivities used to match data in Figure 2 exhibit an anomalous enhanced diffusion at high concentrations in agreement with previous experiments and lattice monte carlo simulations.

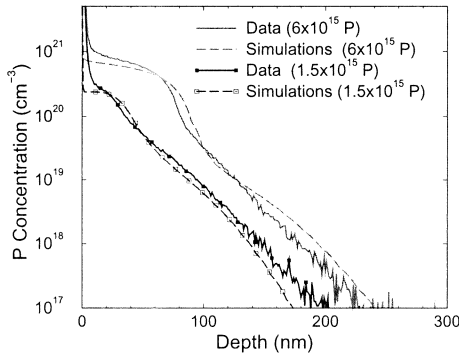


Figure 2: Comparison of simulation (dashes) and experiment (solid) to 1.5×10^{15} – 6×10^{15} cm^{-2} P implanted at 8keV and annealed for 1000°C, 10s. Note the anomalous kink and tail profile.

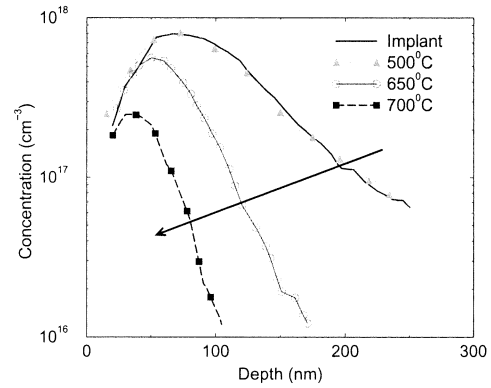


Figure 4: Experimental data from Jeng *et al.* shows anomalous non-gaussian diffusion of fluorine.

[13] M. Diebel and S.T.Dunham *Mat. Res. Soc. Symp. Proc.* **717**, C4.5.1 (2002).

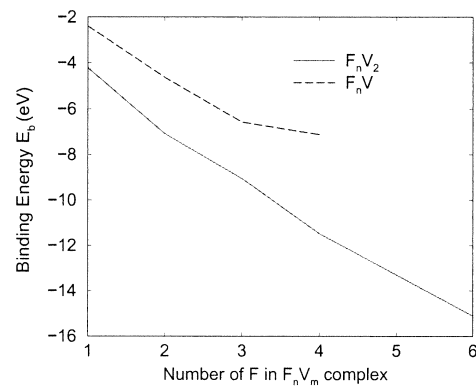


Figure 5: Results from *ab-initio* calculations show strong binding with vacancy clusters indicating fluorine decoration of small vacancy clusters.

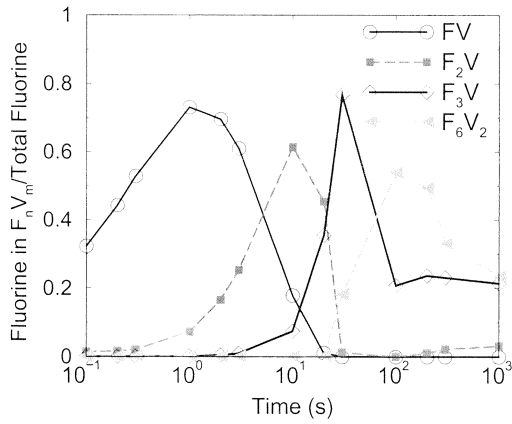


Figure 6: Time evolution of fluorine in the significant fluorine vacancy complexes using the continuum multi cluster model at 650°C. The F_3V complex forms rapidly during the initial stages of the anneal.

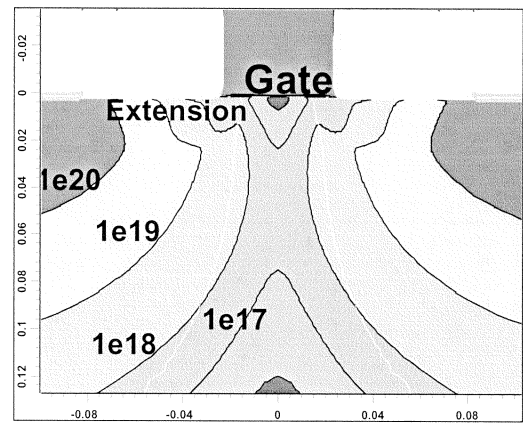


Figure 9: TSUPREM4 Simulation of a NMOS transistor with a gate length of 50nm showing lateral diffusion of phosphorus into the drain extension/channel region.

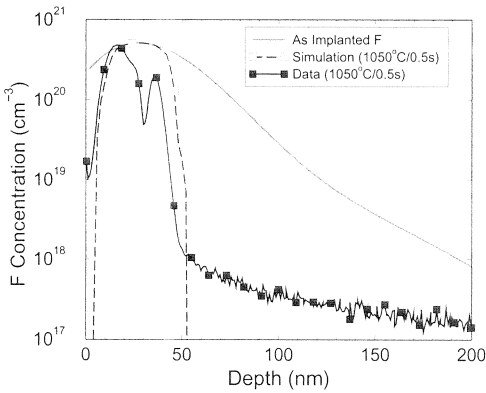


Figure 7: Comparison of simulation (dashes) and experiment (solid) to $3 \times 10^{15} \text{cm}^{-2}$ fluorine implanted at 20keV and annealed for 1050°C/0.5s.

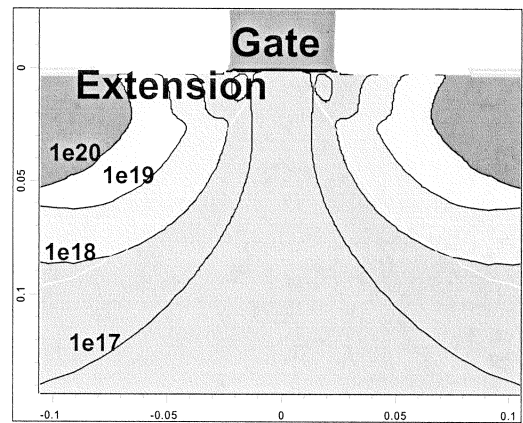


Figure 10: Addition of a Fluorine implant at source/drain leads to retardation of the phosphorus diffusion as shown by the doping contours.

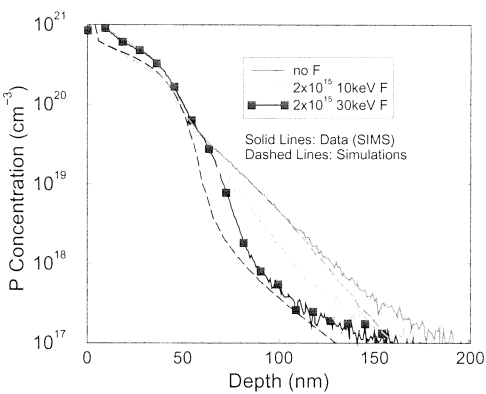


Figure 8: Comparison of simulation (dashes) and experiment (solid) of $4 \times 10^{15} \text{cm}^{-2}$ phosphorus implanted with varying fluorine implant energies and annealed for 1050°C/0.5s.